Arabian Journal for Science and Engineering (2020) 45:4959–4965
https://doi.org/10.1007/s13369-020-04542-2

RESEARCH ARTICLE-PHYSICS

# Synthesis and Mechanical Properties of Zirconia–Yttria Matrices/Alumina Short Fibre Composites

Omyma H. Ibrahim[1] · Kolthoum I. Othman[1] · Ahmed A. Hassan[1] · S. El-Houte[1] · M. El Sayed Ali[1]

Received: 17 November 2019 / Accepted: 16 April 2020 / Published online: 30 April 2020
© King Fahd University of Petroleum & Minerals 2020

**Abstract**

Yttria tetragonal zirconia polycrystals (YTZP)/alumina short fibre ($Al_2O_3$-SF) composites were prepared by wet ball milling. Three different commercial powders of YTZP containing 2, 2.5 and 3 mol% of yttria (denoted as TZ2Y, TZ2.5Y and TZ3YA, respectively) were used as matrices, reinforced with 20 wt% $Al_2O_3$-SF. The effect of sintering conditions on the mechanical properties of the composites was studied. XRD and SEM techniques were used for the characterization of the prepared composites. The fracture toughness and hardness were determined by the Vickers indentation technique. The bend strength was measured using a four-point bending test machine. The results showed that both strength and toughness increase with yttria content. The TZ3YA/20 wt% $Al_2O_3$-SF composite showed bend strengths up to 760 MPa and fracture toughness of 9.2 MPa$\sqrt{m}$ upon pressureless sintering at 1600 °C. Higher values of the bend strength, up to 855 MPa, were obtained for the post-sintered hipped composites at 1500 °C. The high bend strength and fracture toughness, $K_{IC}$, result from strong fibre matrix interface. The toughening mechanisms were found to comprise transformation toughening, domain switching and crack deflection toughening. The addition of $Al_2O_3$-SF to the matrices of low yttria content was invaluable due to its high monoclinic content upon sintering.

**Keywords** Zirconia ceramics · YTZP · Composite · Synthesis · Mechanical properties

## 1 Introduction

Zirconia-based ceramics cover a large area of the advanced technical ceramic materials, due to their unique combination of optical, electrical, mechanical, thermal, and chemical properties, which make it find applications in many fields such as structural materials, thermal barrier coating, solid oxide fuel cell electrolytes [1] and photonic applications [2]. Zirconia has three different crystal structures: monoclinic at room temperature to 1170 °C, tetragonal between 1170 and 2370 °C, and cubic at 2370 °C and higher. By adding stabilizing oxides like CaO, MgO, $CeO_2$, $Y_2O_3$ to pure Zirconia, multiphase materials known as partially stabilized zirconia (PSZ) are generated. Among these, yttria-stabilized tetragonal zirconia polycrystalline (YTZP) ceramics are regarded as strong candidates for structural applications due to their excellent strength and toughness in combination with high wear resistance and chemical inertness. Besides many of implant biomaterials, YTZP ceramics have been increasingly used because of their excellent biocompatibility, low thermal conductivity and superior mechanical properties [1].

At high temperatures, the YTZP ceramics exhibit degradation in their mechanical properties, due to the progressive spontaneous transformation of the metastable tetragonal phase to the monoclinic phase. The addition of a material with high elastic modulus to YTZP forming composites retained its high strength and toughness due to load transfer and crack deflection mechanisms [3].

Several examples have been reported for such composites, YTZP/SiC whiskers [4], YTZP/$Al_2O_3$ fibre [5] and YTZP/$Al_2O_3$ powder [6–8].

Reinforcing with high strength fibres or whiskers affects the strength of the composite depending on various parameters such as the interface properties [9, 10], physical and chemical compatibility [11]. Different processing parameters such as the mixing methods [12, 13], composition [14], shaping [15] and firing conditions [16] could also have a great influence on the composite properties.

✉ Omyma H. Ibrahim
omyma_essam@yahoo.com

1 Metallurgy Department, NRC, Atomic Energy Authority, Cairo, Egypt

The YTZP/$Al_2O_3$ short fibres (YTZP/$Al_2O_3$-SF) belong to the oxide matrix/oxide fibre composites, which are supposed to have good stability against oxidation compared to other systems based on metals or carbides. This material, therefore, seemed attractive to us and is the subject of this study.

In the present work, YTZP/$Al_2O_3$-SF composites have been prepared using a simple mixing method. The physical and mechanical properties are evaluated, and the toughening mechanisms are discussed.

## 2 Experimental

Three different commercial powders of YTZP (Tosoh, Japan), containing 2, 2.5 and 3 mol % of yttria (designated as TZ2Y, TZ2.5Y and TZ3YA, respectively), have been used as matrices. $Al_2O_3$-SF is normally added in amounts ranging from 10 to 30 wt% [17, 18]. Amounts below 10 wt% will not be effective in reinforcing the matrix, while the high content (above 30 wt%) may result in agglomeration that degrades the mechanical properties. So, in the present work 20 wt% $Al_2O_3$-SF (ICI Chemicals, UK) were added to each of the above matrices. For the TZ3YA matrix, an additional mixture containing 10 wt% of $Al_2O_3$-SF was prepared.

Prior to their addition to the matrix, the $Al_2O_3$-SF were dispersed in an aqueous solution at a pH = 2, adjusted by adding few drops of $HNO_3$ and monitored by pH meter. This process enabled rapid sedimentation of large fibres and agglomerates to get rid of, thus avoiding non-homogeneity in the composite. The suspension containing the remaining dispersed short fibres was dried. The selected fibres had a diameter of about 2 µm, measured using a transmission optical microscope, and about 10 aspect ratio. The required amount of short fibres, for each composite, was dispersed in a small amount of aqueous solution at pH = 2. It was then added to an ethanol solution containing the YTZP powders. The mixing was performed in a ball mill using plastic balls, at a moderate speed for 20 h. In this way, the reduction of short fibre aspect ratio which might be caused by milling was minimized. After mixing, the resulting slurry was oven-dried, and the powder was then sieved and pressed at 100 MPa in a steel die of dimensions 8 × 35 mm using a compact type hydraulic press.

The compacts were pressureless-sintered, in air ($MoSi_2$ furnace), at different temperatures: 1400, 1500, 1600 and 1650 °C for 2 h. Some of the pressureless-sintered (at 1400 °C) composite pellets were hot isostatically pressed (hipped) at 1500 °C/1 h at a pressure of 100 MPa. The apparent densities of the sintered pellets were determined by Archimedes method (water displacement method) in which a fully submerged pellet in water displaces the same amount of water as its volume. Dividing the pellet dry weight by this volume gives the density according to following equation:

$$\rho = \left(\frac{m_o}{m_1 - (m_2 - m_{\mathrm{w}})}\right) \times \rho_{\mathrm{water}}$$

where $\rho$ is the sintered density, $m_{\mathrm{o}}$ is the dry weight, $m_1$ is the wet weight in air, $m_2$ is the wet weight suspended in water, $m_{\mathrm{w}}$ is the weight of wire (used to suspend the pellets in water) suspended in water and $\rho_{\mathrm{water}}$ is the water density.

The fracture toughness and hardness were determined on the polished sample surfaces by the Vickers indentation technique, using a Zwick hardness tester at loads ranging from 50 to 200 N. The bend strength was measured using a four-point bending test machine with 20 mm supporting and 10 mm loading spans and a cross head speed of 0.22 mm/min. The phases present in the sintered samples were determined using Toraya's formula [19] from XRD patterns obtained using XRD machine (XRD-3A Shimadzu–Japan). The microstructure was examined using SEM (JSM5400).

## 3 Results and Discussion

### 3.1 Densification Behaviour

#### 3.1.1 Pressureless Sintering

The sintered densities of the composite compacts made from TZ3YA matrix having 10 and 20 wt% $Al_2O_3$-SF fired at different temperatures for 2 h are shown in Fig. 1. It can be seen that sintering at 1500 and 1650 °C produces highly dense ceramic composites. The high densities obtained could be attributed to the removal of the larger size $Al_2O_3$-SF and the short fibre agglomerates, besides the excellent homogeneity obtained by the mixing in suspension, as can be seen from the SEM micrograph (Fig. 2).

The composite containing 20 wt% $Al_2O_3$-SF showed slightly better densification (~ 100% of TD) than that containing 10 wt%, which is in agreement with the results reported by Bream, 1989 [20] and relatively higher than those obtained by Pujari & Jawed 1986 [5]. This might be due to the difference in the diameter of the reinforcing fibres which was 2 µm in our case compared to 20 µm for the later.

#### 3.1.2 Hot Isostatic Pressing

Post-sintering hot isostatic pressing at 1500 °C, 100 MPa for 1 h of the composite compacts containing 20 wt% $Al_2O_3$-SF, pre-sintered at 1400 °C, yielded an increase in their densities from ~ 92% to almost 100% of the theoretical values.

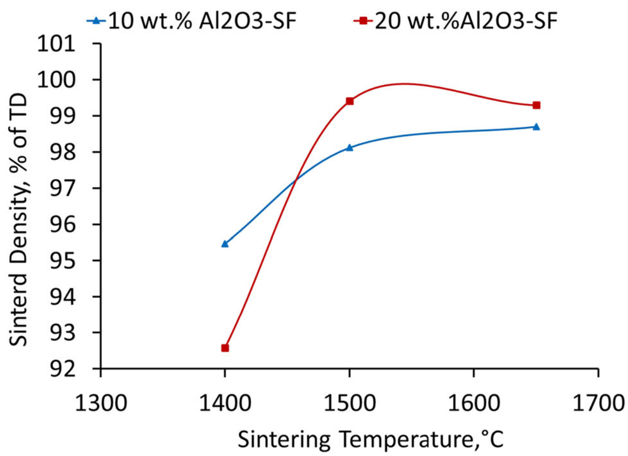


**Fig. 1** The sintered densities versus sintering temperatures for TZ3YA/$Al_2O_3$-SF composites

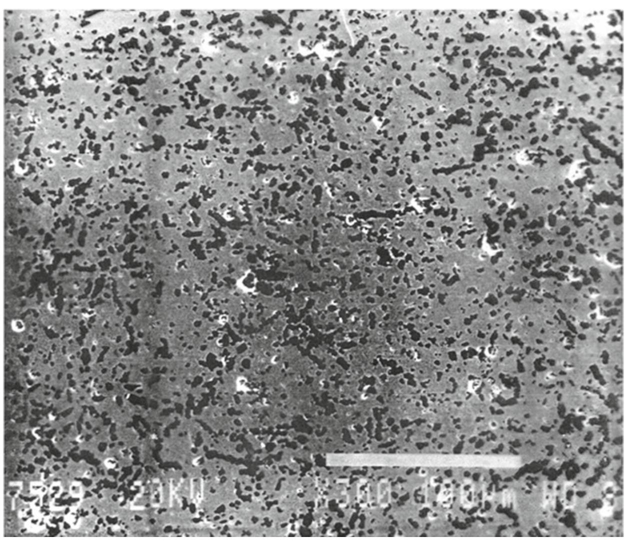

**Fig. 2** SEM micrograph of a polished section of TZ3YA (grey)/20 wt% $Al_2O_3$-SF (dark) sintered in air at 1650 °C/2 h

## 3.2 Mechanical Properties

### 3.2.1 Effect of Sintering Conditions and Fibre Content

The bend strengths versus sintering temperatures for TZ3YA/$Al_2O_3$-SF, pressureless-sintered, composites are shown in Fig. 3. From the figure, bend strengths of 694 and 760 MPa were obtained upon sintering at 1600 °C/2 h for the composites containing 10 and 20 wt% $Al_2O_3$-SF, respectively. The fracture toughness measured for the same composites was found to be 9 and 9.2 MPa$\sqrt{}$m, respectively. These values are nearly twice the values measured for the TZ3YA matrix (bend strength of 380 MPa and fracture toughness of 5.96 MPa$\sqrt{}$m), upon sintering at the same temperature.

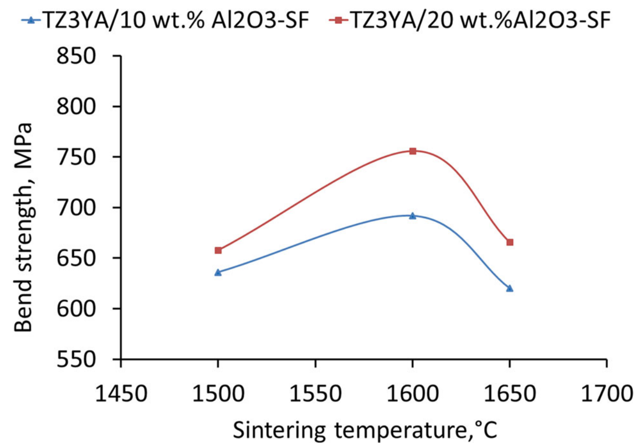


**Fig. 3** Bend strength versus sintering temperature for TZ3YA/Al2O3-SF Composites

**Table 1** Bend strengths ($\sigma$) and Weibull modulus ($m$) of the TZ3YA composites, pressureless-sintered at 1400 °C and hipped at 1500 °C/1 h

| Sintering method | 10% fibre | | 20% fibre | |
|---|---|---|---|---|
| | $\sigma$ (MPa) | $m$ | $\sigma$ (MPa) | $m$ |
| Pressureless sintering | 639 | 4.1 | 661 | 46.8 |
| Hipped | 735 | 9.6 | 855 | 18.3 |

The strengthening effect of the alumina short fibres might be attributed to load transfer contribution from a strong TZ3YA/$Al_2O_3$-SF interface, in agreement with a previous interpretation in the YTZP/SiC whisker system [3]. However, the increase in the strength with short fibre addition in the present work is relatively smaller than that observed in the case of TZ3Y/SiC whisker composites prepared by hot pressing. This might be attributed to the whisker alignment, being preferentially normal to the hot pressing direction in the latter case, while randomly oriented in the former.

The TZ3YA composites containing 10 and 20 wt% $Al_2O_3$-SF, hipped at 1500 °C/100 MPa for 1 h, showed an increase in the bend strength of 100 and 200 MPa above the values obtained for the pressureless-sintered composites, respectively (Table 1). The increase in the short fibre content was accompanied with a substantial increase in the Weibull modulus (m) obtained from the bend strength measurements. However, this increase in strength due to hipping was accompanied by a slight decrease in fracture toughness and an increase in hardness as given in Table 2.

### 3.2.2 Effect of Yttria Content in the Zirconia Matrix

Figure 4 shows bend strength and the fracture toughness versus yttria content for composites having 20 wt% $Al_2O_3$-SF, pressureless-sintered at 1650 °C/2 h. It can be seen that both strength and toughness increase with yttria content. The low

**Table 2** Fracture toughness ($K_{IC}$) and hardness (Hv) of the TZ3YA composites pressureless-sintered at 1400 °C and hipped at 1500 °C/1 h

| Sintering method | 10% fibre | | 20% fibre | |
|---|---|---|---|---|
| | $K_{IC}$ (MPa$\sqrt{m}$) | Hv (GPa) | $K_{IC}$ (MPa$\sqrt{m}$) | Hv (GPa) |
| Pressureless | 5.4 | 13.1 | 5.8 | 13.2 |
| Hipped | 4.9 | 13.6 | 5.2 | 13.9 |

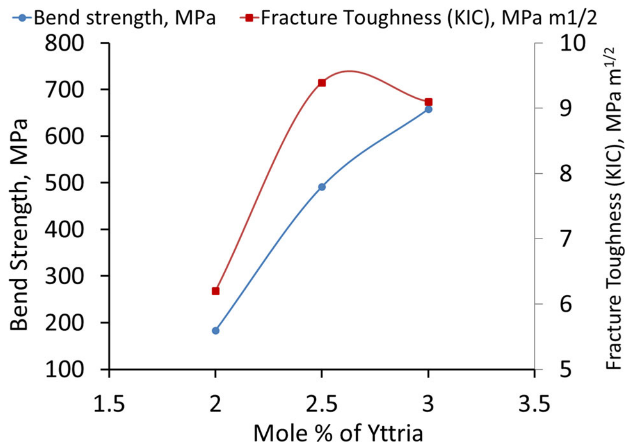


**Fig. 4** Bend strength and the fracture toughness versus yttria content for 20 wt% $Al_2O_3$-SF composites, pressureless-sintered at 1650 °C/2 h

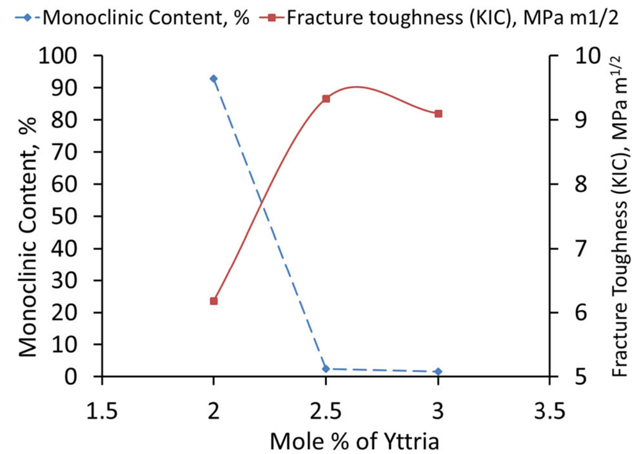


**Fig. 6** Monoclinic content and the fracture toughness versus the yttria content in the matrices of composite containing 20 wt% $Al_2O_3$-SF

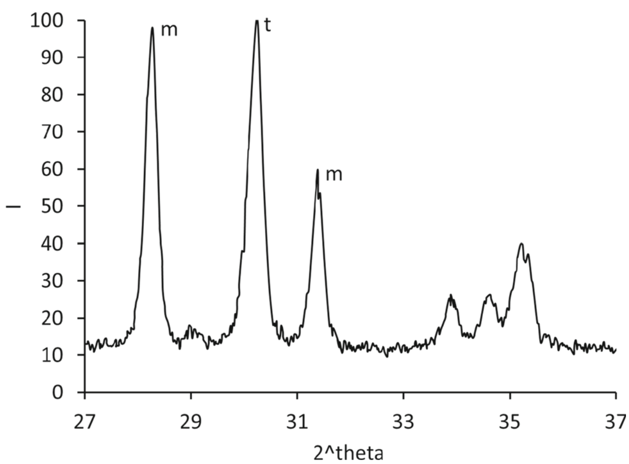


**Fig. 5** XRD pattern of the TZ2Y/20 wt% $Al_2O_3$-SF composite

strength and toughness values obtained for the composite containing 2 mol% yttria (TZ2Y) are attributed to the large amount of the monoclinic phase (about 90%), generated as a result of tetragonal to monoclinic phase transformation during cooling, on the sintered surface of the composite (Fig. 5). The large number of microcracks generated by such ubiquitous transformation could be the cause of its poor mechanical properties. In contrast, the good mechanical properties obtained for the composites made from the 2.5 and 3 mol% yttria YTZP matrices might be due to the absence of monoclinic phase on the sintered surface as can be seen from Fig. 6.

### 3.2.3 Effect of Sample Surface Preparation

It is well known that the crack propagation in fibre composites depends largely on the orientation of the reinforcing fibres. Consequently, for such composites with randomly oriented short fibres, one should expect a high degree of anisotropy in crack lengths emerging from the corners of the Vickers indentation as that made on the polished surface of TZ3YA/20 wt% $Al_2O_3$-SF, sintered at 1600 °C, shown in Fig. 7a. The surface has been subjected to rough grinding to remove the as sintered surface layer prior to polishing, which resulted in random orientation of fibres. It can be seen that larger cracks emerged from left and upper corners, while shorter ones emerged from the right and lower corners.

In contrast, careful grinding using a light force for a short time followed by polishing did not remove the well-aligned fibres in the sample's outer surface layer as shown in Fig. 7b. In this case, very small cracks emerged from the corners of the Vickers indentation. This shows the effect of fibre alignment on suppressing the crack propagation and gives evidence that the fibres are aligned only at the outer sample's surface in the plane normal to the pressing direction.

Consequently, a substantial improvement in both fracture toughness and strength could be achieved by using hot pressing which might help in massive alignment of the fibres in normal planes to the pressing direction.

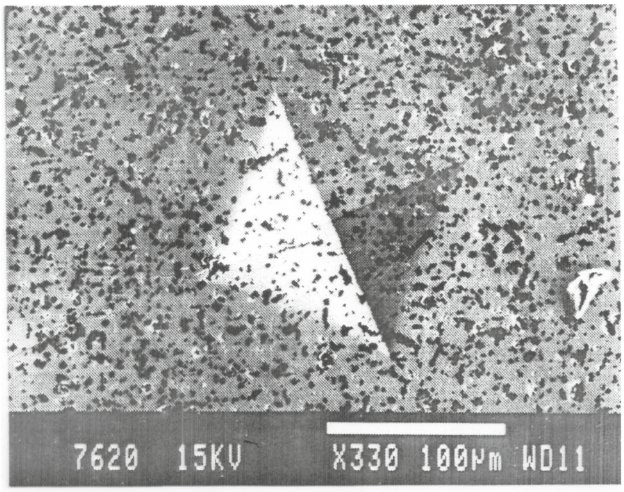


**(a)**

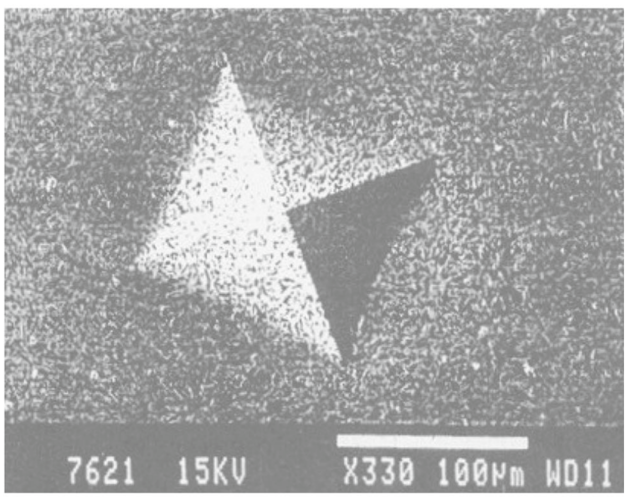


**(b)**

**Fig. 7** Vickers indentation on the polished surface of TZ3YA (grey)/20 wt% $Al_2O_3$-SF(dark) composites

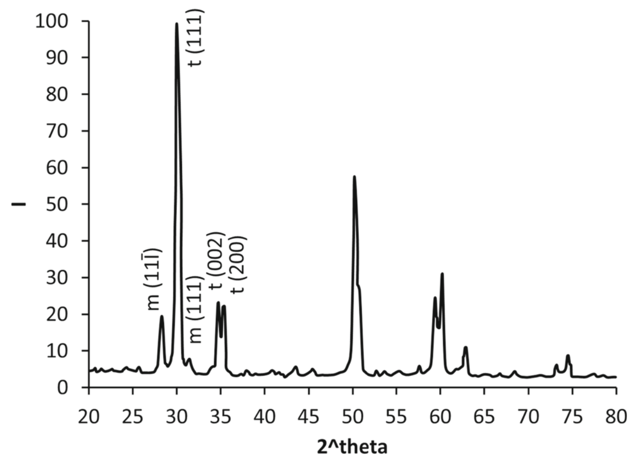


**Fig. 8** XRD pattern made on the cut surface of TZ3YA/20 wt% $Al_2O_3$-SF composite sintered at 1650 °C/2 h

### 3.3 Toughening Mechanisms

Three toughening mechanisms are supposed to play role in the toughening of the TZ3YA/$Al_2O_3$-SF composites. The first one is transformation toughening, due to the tetragonal to monoclinic phase transformation, that occurs ahead of the propagating crack tip associated with stress application on the composite. The second is the stress assisted matrix domain switching toughening, which is related to the change from one equilibrium state to another by domain reorientation. This is expressed by the increase in the intensity of the line (002) and a decrease in the intensity of line (200), as shown in Fig. 8 of the XRD pattern made on the composite cut surface. The contribution of the ferro-elastic domain switching to the stress intensity factor $K_{IC}$ was approximately estimated to be in the order of 2 MPa$\sqrt{m}$, for tetragonal zirconia ceramics [21].

The third is the toughening due to the reinforcing fibres, where a crack deflection mechanism might take place. It can be seen that the crack directed towards the $Al_2O_3$ fibre is deflected along the fibre/matrix interface as shown in Fig. 9a. In this figure, it can be seen that the principle crack emerging from the Vickers indentation corner has been obstructed by a fibre oriented normal to its propagation direction. The fracture energy is dissipated through the lateral crack which is in turn subjected to crack deflection at the fibre/matrix interface as shown in Fig. 9b. Figure 10 shows the intergranular propagation of a crack emerging from the indenter corner which firstly did not meet a well oriented fibre, but later met one and was arrested.

The interfaces between the matrix and the fibres are a critical play maker in the fibre composite manufacture; fibre coating is necessary to form a bond layer [21]. Whenever the interface layers have high bond strength, they will act as load transfer media between the matrix and the strong fibre, which enhances both fracture toughness and strength of the composite. The strong bonding between fibre/matrix rules out the harmful effects resulting from fibre debonding. The SEM micrograph in Fig. 11 shows a white thin glassy phase (interface) layer between a grey TZ3YA matrix and a black $Al_2O_3$ fibre. This layer of glassy phase plays the role of the strong bonding interface.

## 4 Conclusions

- Highly dense (about 98% of TD) YTZP/$Al_2O_3$-SF composites with excellent distribution of alumina short fibre were prepared using a simple mixing technique.

**(a)** TZ3YA (gray)/10 wt.% $Al_2O_3$-SF (dark)

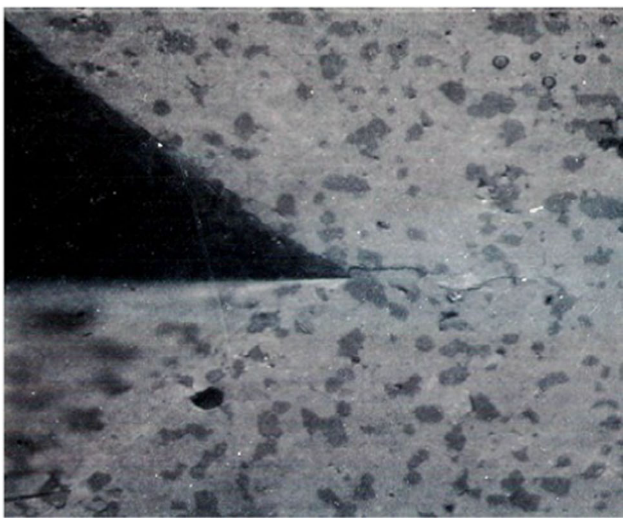

**(b)** TZ3YA (gray)/20 wt.% $Al_2O_3$-SF (dark)

**Fig. 9** Optical micrographs of Vickers indentation on composites' polished surfaces, sintered at 1650 °C/2 h (780X)

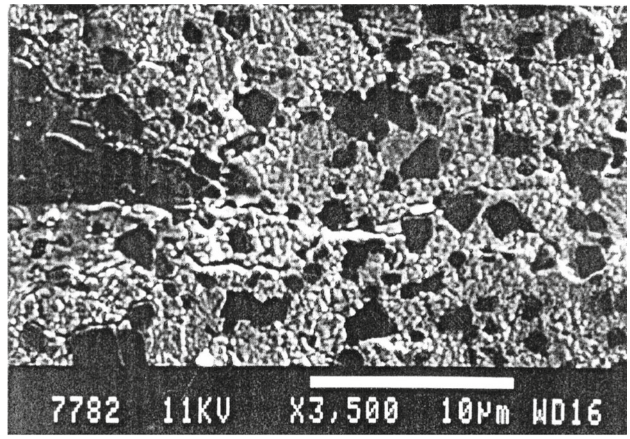


**Fig. 10** SEM micrograph showing intergranular crack deflection in TZ3YA (grey)/20 wt% $Al_2O_3$-SF (dark) composite sintered at 1650 °C/2 h

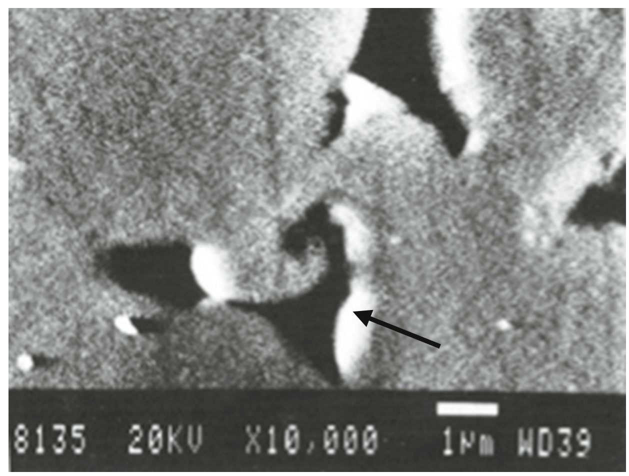


**Fig. 11** SEM micrograph showing a glassy phase layer (indicated by arrow) in TZ3YA/20 wt% $Al_2O_3$-SF composite

- An increase in the $Al_2O_3$-SF content increases both the bend strength and toughness.
- The pressureless-sintered TZ3YA composites containing 20 wt% $Al_2O_3$-SF showed high strength and fracture toughness values up to 760 MPa and 9.2 MPa$\sqrt{m}$, respectively, compared to 380 MPa and 5.96 MPa$\sqrt{m}$ for the TZ3YA matrix.
- The TZ3YA/$Al_2O_3$-SF composites hipped at 1500 °C/100 MPa for 1 h showed an increase in the bend strength of 100 and 200 MPa above the values obtained for the pressureless-sintered TZ3YA-composites containing 10 and 20 wt% $Al_2O_3$-SF, respectively.
- Much lower values of bend strength and toughness (250 MPa and 5.5 MPa$\sqrt{m}$) were obtained for the composite with low percentage of the stabilizing yttria, TZ2Y/20 wt% $Al_2O_3$-SF, due to the high percentage of the monoclinic phase formed on the sample surface upon sintering.
- A thin glassy phase was found to exist between fibre/matrix, forming a strong interface.
- The mechanisms of toughening consist of simultaneous contribution of transformation toughening, domain switching toughening and crack deflection around alumina strong fibres.

## References


1. Thakare, V.: Progress in synthesis and applications of zirconia. Int. J. Eng. Res. Dev. **5**(1), 25–28 (2012)
2. Marcaud, G.; Matzen, S.; Alonso-Ramos, C.; Le Roux, X.; Berciano, M.; et al.: High-quality crystalline yttria-stabilized-zirconia thin layer for photonic applications. Phys. Rev. Mater. Am. Phys. Soc. **2**(3), 35202 (2018)

3. Yasuda, E.; Kimura, S.: Mechanical properties of SiC whisker-reinforced PSZ. Adv. Ceram. **24**, 701–707 (1988)
4. Anggraini, L.: Fracture behaviour of SiC–$ZrO_2(Y_2O_3)$ green composite with harmonic microstructure. Int. J. Mech. Mechatron. Eng. IJMME-IJENS **16**(03), 159–165 (2016)
5. Pujari, V.; Jawed, I.: The alumina fibre/tetragonal zirconia polycrystals composite system. Composites **17**(2), 137–140 (1986)
6. Tsukma, K.; Ueda, K.: Strength and fracture toughness of isostatically hot pressed composites of $Al_2O_3$ and $Y_2O_3$-partially stabilized $ZrO_2$. J. Am. Ceram. Soc. **68**, C4–C5 (1985)
7. Ali, M.E.-S.; El-Houte, S.; Sørensen, O.T.: Preparation and mechanical properties of ceria doped tetragonal zirconia/alumina ceramics. In: Bentzen J. et al. (eds.) Proceedings of the 11th Risø International Symposium on Metallurgy and Material Science, pp. 263–267 (1990)
8. Al-Mahdy, Y.F.; Eltayeb, H.E.: The effect of nano-$ZrO_2$ and nano-Al-$_2O_3$ reinforcement on flexural and impact strength of repaired acrylic denture base. Al-Azhar Dent. J. **5**(1), 89–100 (2018)
9. Kerans, R.; Hay, S.; Pagano, N.: The role of the fibre-matrix interface in ceramic composites. Ceram. Bull. **68**(2), 429–441 (1989)
10. An, J.; Zhao, J.; Su, Z.G.; Wen, Z.; Xu, D.S.: Microstructure and mechanical properties of ZTA ceramic-lined composite pipe prepared by centrifugal-SHS. Arab. J. Sci. Eng. **40**, 2701–2709 (2015)
11. Davidge, R.: Fibre-reinforced ceramics. Composites **18**(2), 92–98 (1987)
12. Momohjimoh, I.; Hussein, M.A.; Al-Aqeeli, N.: Recent advances in the processing and properties of alumina-CNT/SiC nanocomposites. Nanomaterials **9**(86), 2–41 (2019)
13. Muhammad, R.; Kumar, B.; Chaskar, A.: Synthesis, characterization and mechanical properties of alumina–zirconia nanocomposite particles. J. Mech. Civ. Eng. IOSR-JMCE **14**(3), 40–46 (2017)
14. Gommeringer, M.A.; Kern, F.; Gadow, R.: Enhanced mechanical properties in ED-machinable zirconia–tungsten carbide composites with yttria–neodymia co-stabilized zirconia matrix. Ceramics **1**, 26–37 (2018)
15. Lio, S.; Watanabe, M.; Matsubara, M.; Matsu, Y.: Mechanical properties of alumina/silicon carbide whisker composite. J. Am. Ceram. Soc. **72**(10), 1880–1884 (1989)
16. Tiegs, T.; Becher, P.: Sintered $Al_2O_3$-SiC-whisker composites. Ceram. Bull. **66**(2), 339–342 (1987)
17. Kelles, Ö. G.: Production and Characterization of Alumina Fibre Reinforced Squeeze Cast Aluminum Alloy Matrix Composite. MSc, Thesis Submitted to the Graduated School of Material and Applied Science of Middle East-Technical University (2008)
18. Naskar, M.K.; Basu, K.; Chatterjee, M.: Sol–gel approach to near-net-shape oxide-oxide composites reinforced with short alumina fibers—the effect of crystallization. Ceram. Int. **35**, 3073–3079 (2009)
19. Toraya, H.; Yoshimura, M.; Somiya, S.: Calibration curve for quantitative analysis of monoclinic-tetragonal $ZrO_2$ system by X-ray diffraction. J. Am. Ceram. Soc. **67**, 119–121 (1984)
20. Bream, C.: Preparation of the Alumina Short Fibre/Zirconia Matrix Composite System. Risø-I-456 (1989)
21. Chevalier, J.: What future for zirconia as a biomaterial? Biomaterials **27**, 535–543 (2006)